UDC 616.831.5 + 616.858 + 612.822

Spatial clustering of substantia nigra astrocytes analyzed in rotenone model of hemiparkinsonism

A.G. Nikonenko

Bogomoletz Institute of Physiology, National Academy of Sciences of Ukraine, Kyiv, Ukraine;
e-mail: agn@biph.kiev.ua

This paper addresses spatial aspects of reactive astrogliosis in the substantia nigra pars compacta (SNc) of the rat brain observed 40 and 70 days after the intracerebral 12 μg rotenone infusion. The infusion was shown to cause a marked increase in astrocyte density at both analyzed time points. Minimal spanning tree (MST) analysis was applied to analyze spatial patterns formed by nigral astrocytes. Spatial clusters of these cells, identified as disjoint MST subgraphs, were more numerous in the infused SNc tissue as compared with the control one. Size and density of clusters were significantly different between the infused and control areas 40 and 70 days after the infusion. In conclusion, the data suggests that rotenone-related astrogliosis in the substantia nigra includes changes in spatial patterns of astrocytes as well as transient spatial clustering of these cells.
Key words: astrocytes; Parkinson's disease; rotenone; spatial clustering.

INTRODUCTION

Parkinson's disease (PD) is a multifactorial disorder, and aberrant functioning of the immune system is proposed as an important factor of PD-related neurodegeneration [1]. There are innate immune cells residing in the brain tissue, namely astrocytes and microglia. Star-shaped astrocytes amount to approximately 30% of the total number of cells in mammalian brains and serve a lot of vital roles [2]. Recent evidence suggests astrocytes are involved in PD pathogenesis. Experiments in a mouse model of PD induced by 1-methyl-4-phenyl-1,2,3,6-tetrahydropyridine have shown that exposure of astrocytes to the cytokines IL-1, TNF and complement C1q converted them into neurotoxic cells [3]. It should be noted that proinflammatory cytokines as well as astrocytic calcium-binding protein S100b are present at high levels in the CSF and brain tissue of PD patients [4]. Experimental models of PD can serve as important platforms to study cellular mechanisms of the disease, in particular the role of astrocytes in the early phases of neurodegeneration. Because spatial aspects of nigral astrogliosis remain poorly understood, the aim of this study was to analyze spatial clustering of astrocytes in the rotenone model of hemiparkinsonism.

METHODS

Spatial patterns formed by nigral astrocytes were analyzed in adult male Wistar rats (250-300 g) 40 and 70 days after these animals were infused intracerebrally with 12 μg of rotenone into the left substantia nigra pars compacta (SNc). The procedure of the infusion was described in detail earlier [5]. Seven animals per each experimental group were studied, 14 rats in total. At the end of the experiment, rats were anesthetized, and transcardially perfused with 4% formaldehyde and 2.5% glutaraldehyde in 0.1 M phosphate buffer (pH 7.4). Their brains were removed and cut into 200-μm-thick transverse slices, which were kept in the same fixative for 1.5 hs, and postfixed in 1% OsO_4. Tissue slices were then dehydrated in an ascending series of ethanol followed by dry acetone and embedded in Epon resin (Epon 812, "Sigma", USA).

Semithin 1-μm-thick sections were made using ultramicrotome ("LKB", Sweden) and stained with 1% solution of toluidine blue. Microphotos of SNc tissue on the infused side and respective contralateral side (control area) were made using XSP-13a microscope ("Nanbei", China) equipped with a digital camera at 40× objective magnification. For astrocytes, density of cell bodies (AD) and their spatial clusters (AcD) were quantified by counting objects for a sample area and expressed as objects/10000 μm^2. Minimal Spanning Tree (MST) analysis was used to quantify spatial patterns formed by astrocytes. A custom-made software written in "Delphi" (Version 7, "Borland Software Corporation", USA) was applied to run a MST algorithm using coordinates of cell profile centroids as an input. The coordinates were measured with an "ImageJ" open source software (version 1.51j8, National Institutes of Health, USA) in digital micrographs. First, a MST graph was constructed on a set of centroids for all objects of interest observed within a digital micrograph (Fig. 1B). Then, MST edges having lengths greater of a threshold value (i.e., 30 μm) were removed (Fig. 1C). Disjoint MST subgraphs left were considered to indicate spatial clusters of astrocytes. Individual values of MST edge length (EL_{MST}) were pooled per an experimental group. Statistical analysis was performed using open source Power Statistics software for Linux. Values are shown as mean ± standard error of the mean. The nonparametric two-tailed Kolmogorov-Smirnov test was used to assess the differences between samples. $P < 0.01$ was considered statistically significant.

RESULTS

Visual inspection of SNc tissue revealed groups of medium-sized, multipolar neurons scattered in neuropil. Occasionally, astrocytes were observed in the tissue, being easily identified by their characteristic round nuclei (Fig. 1A). The infusion of rotenone led to more than 30% increase in AD value after 40 days, up to 3.49 ± 0.13 cells/10000 μm^2, with respect to the control value, 2.60 ± 0.12 cells/10000 μm^2 on the contra-lateral side ($P < 0.01$). 70 days after the

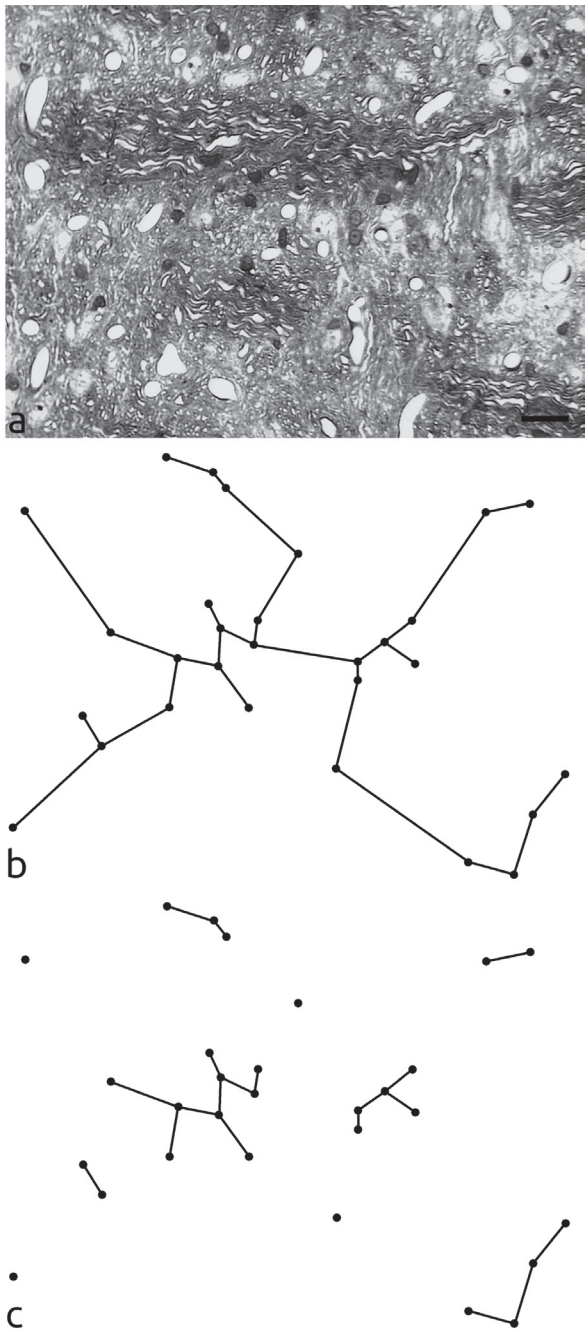

Fig. 1. A representative micrograph illustrating the SNc tissue 70 days after the 12 μg rotenone infusion, on the infused side, scale bar = 20 μm (A). A MST graph built on the centroids of astrocyte profiles (B). Disjoint MST subgraphs revealed after decomposing MST shown in B, with threshold value of 30 μm (C)

infusion AD equalled 3.45 ± 0.16 cells/10000 μm^2 on the infused side versus the control value of 2.58 ± 0.14 cells/10000 μm^2 ($P < 0.01$). The data indicates that the increase in AD takes place within 40 days after the rotenone infusion, AD value not changing essentially afterwards.

In order to detail rotenone-related changes in AD we applied MST analysis. The infusion of rotenone caused, after 40 days, 16% decrease in EL_{MST} value, down to 36.1 ± 0.9 μm (n = 501) with respect to the control value, 43.3 ± 1.6 μm (n = 281) ($P < 0.01$). 70 days after the infusion EL_{MST} equalled 38.3 ± 0.9 μm (n = 480) on the infused side versus the control value of 44.7 ± 1.6 μm (n = 257), on the contra-lateral side ($P < 0.01$; Fig. 2). Together, the data reveals lower EL_{MST} values on the infused side as compared with the control ones, at both time-points analyzed. These quantities are in accord with AD changes. According to the natural logic, the more astrocytes are observed within a defined area, the closer they are to one another.

However, EL_{MST} parameter itself tells little

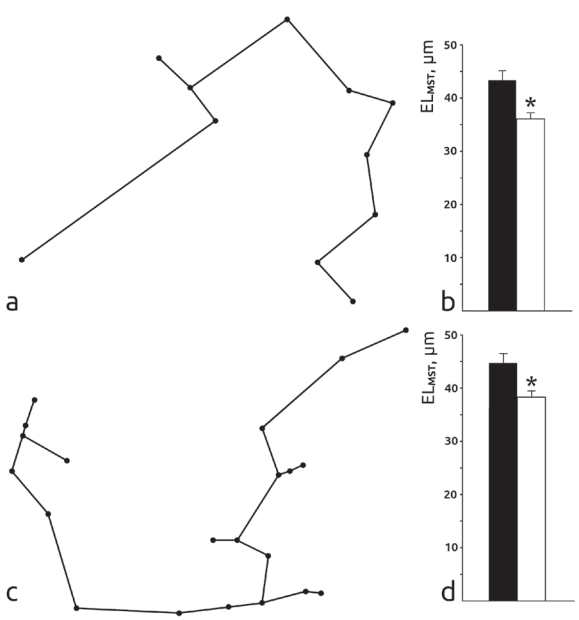

Fig. 2. MST graphs built on representative micrographs of the SNc tissue taken 40 days after the rotenone infusion, on the control side (A) and infused side (C). EL_{MST} on the control side (filled black bars) and infused side (open bars) 40 (B) and 70 (D) days after the infusion

of spatial clustering. That is why in order to analyze the latter MST algorithm was modified allowing to remove individual edges longer of a selected threshold value (i.e., 30 μm). Then, clusters of astrocytes were revealed and analyzed. The infusion of rotenone led after 40 days to more than 40% increase in AcD value, up to 0.79 ± 0.05/10000 μm^2 with respect to the control value, 0.55 ± 0.05/10000 μm^2 ($P < 0.01$). 70 days after the infusion AcD equalled 0.74 ± 0.05/10000 μm^2 in the infused area versus the control value of 0.52 ± 0.08/10000 μm^2 ($P < 0.01$). Together, the data shows that AcD was higher on the infused side than on the control one at both time-points analyzed.

To analyze the propensity of astrocytes to group together, cluster size was selected as a proxy measure. The analysis has shown that 40 days after the infusion 2- and 4-cell clusters were less frequent and 3-, 5- and 6-cell ones – more frequent on the infused side as compared with the control side (Fig. 3B). 70 days after the infusion, 2-, 5- and 6-cell clusters were less frequent, while 3-, and 4-cell clusters were more frequent in the infused area as compared with the control one (Fig. 3D). Our interpretation of these data is that the rotenone-dependent astrogliosis is associated with pronounced changes in the spatial arrangement of astrocytes. These cells become more numerous in the affected SNc area where they form transient spatial clusters.

DISCUSSION

Serving a number of vital roles in the brain, astrocytes respond to brain tissue impairments by a transformation commonly known as reactive astrogliosis. The intensity of this transformation varies depending on the severity of a CNS insult [6, 7]. Important roles played by astrocytes entail their specific spatial arrangement in the brain tissue. They are sparse in areas with a high density of neuronal cell bodies, being replete in areas full of dendrites and axons [8]. In the postnatal brain, new astroglial cells originate, most probably, from differentiated astrocytes

[9]. As these cells function as a network one would expect that their collective reaction to tissue impairments could presume changes in their spatial arrangement.

In this study, MST analysis was applied to found whether such changes are associated with the formation of spatial clusters of astrocytes. MST is the shortest network of line segments interconnecting a set of given points (e.g., object centroids) without a closed path. The mean and standard error of the mean of a line segment length sample provide quantities to characterize a given spatial pattern. MST was selected among other tools because it has no border effects typical of Voronoi diagrams and, in contrast to the nearest-neighbor distance distribution, takes into account distances to all members of a spatial set. MST technique was applied earlier to analyze gene expression patterns [10], trace neurons [11] and quantify spatial arrangement of filamentous structures [12]. In this particular case a MST graph was first constructed on a set of cell body centroids for all astrocytes observed within the test window. Then, those MST edges, whose lengths were greater of a threshold value, were removed. Finally, MST subgraphs left, comprising at least two connected points, were considered to indicate astrocyte clusters. As one can observe, when threshold value equals zero, each cell represents a cluster. With the maximum threshold value all cells lie within a single cluster. A threshold value equal to 30 μm was selected on an empirical basis taking into account that the cell body of an astrocyte spans 10-20 μm and its processes radiate out for another 20-30 μm.

Results have shown that rotenone infusion caused a rise in the density of astrocytes. Our earlier data provided evidence that this effect is due to rotenone and is not related to the mechanical injury of the tissue, procedure or influence of diluting medium, dimethyl sulphoxide [13]. Growing numbers of astrocytes in the affected SNc tissue may be explained by their proliferation. MST analysis broadly confirmed AD changes. EL_{MST} values were significantly lower in the infused regions with respect to the control ones ($P < 0.01$) demonstrating that astrocytes are closer to one another in the affected area.

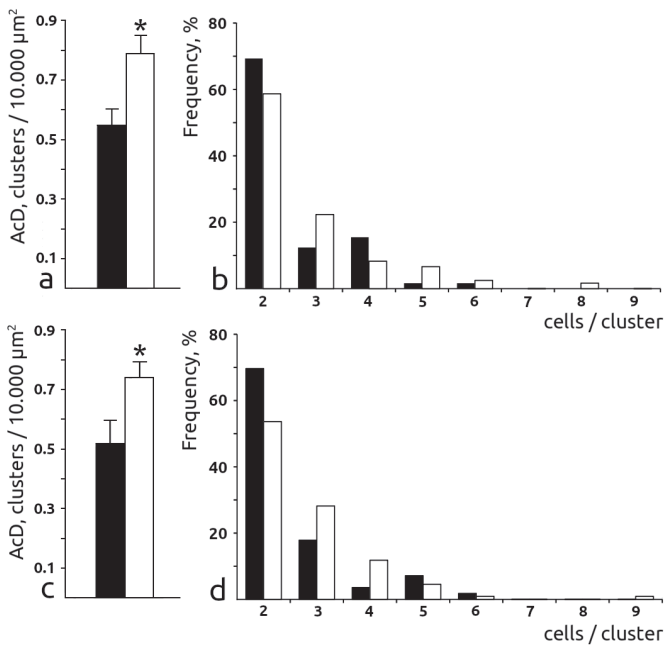

Fig. 3. Density of astrocyte clusters (AcD) (A, C) and MST cluster size distributions (B, D) on the control side (filled black bars) and infused side (open bars) 40 (A, B) and 70 (C, D) days after the infusion

Deconstruction of MSTs into subgraphs allowed to reveal spatial clusters of astrocytes. Density of these clusters was higher in the infused zones with regard to the control regions. In addition, cluster size distribution was affected by the infusion, being different between the experimental and control areas of SNc tissue, at both time points analyzed. It is interesting that cluster size was distributed differently 40 and 70 days after the rotenone infusion showing a transient nature of these clusters. Additional studies are necessary to thoroughly understand dynamics of astrocyte clustering,

CONCLUSIONS

The intracerebral 12 μg rotenone infusion leads to degeneration of neurons and related astrogliosis in the infused regions of the SNc tissue. Local population of nigral astrocytes reacts to this tissue impairment by growing in numbers and changing spatial arrangement of individual cells. Transient clustering of nigral astrocytes revealed by MST analysis provides important details about cellular mechanisms underlying repair and adaptive plasticity of the brain tissue.

The author of this study confirms that the research and publication of the results were not associated with any conflicts regarding commercial or financial relations, relations with organizations and/or individuals who may have been related to the study.

А.Г. Ніконенко

АНАЛІЗ УТВОРЕННЯ ПРОСТОРОВИХ КЛАСТЕРІВ АСТРОЦИТІВ ЧОРНОЇ СУБСТАНЦІЇ В УМОВАХ РОТЕНОНОВОЇ МОДЕЛІ ГЕМІПАРКІНСОНІЗМУ

Інститут фізіології ім. О.О. Богомольця НАН України, Київ; e-mail: agn@biph.kiev.ua

Досліджували просторові аспекти реактивного астрогліозу у компактній частині чорної субстанції (ЧСк) головного мозку щура через 40 та 70 днів після внутрішньомозкової інфузії ротенону у дозі 12 мкг. Показано, що інфузія ротенону викликала помітне підвищення щільності астроцитів у обох досліджених термінах. Просторовий розподіл астроцитів чорної субстанції аналізували, використовуючи метод мінімального охоплюючого дерева (МОД). Просторові кластери цих клітин, які визначали як окремі підграфи МОД, були більш численними в інфузованій зоні ЧСк порівняно з контрольною. Розмір та щільність кластерів суттєво відрізнялися в цих зонах через 40 та 70 діб після інфузії. Таким чином, отримані результати вказують на те, що ротенонзалежний астрогліоз у чорній субстанції включає зміни у просторовому розподілі астроцитів, а також формування тимчасових просторових кластерів цих клітин.

Ключові слова: астроцити; хвороба Паркінсона; ротенон; просторові кластери.

REFERENCES

1. Holmans P, Moskvina V, Jones L, Sharma M, Vedernikov A. A pathway-based analysis provides additional support for an immune-related genetic susceptibility to Parkinson's disease. Hum Mol Genet. 2013;22 (5):1039-49.
2. Tsai HH, Li H, Fuentealba LC, Molofsky AV, Taveira-Marques R, Zhuang H, Tenney A, Murnen AT, Fancy SP, Merkle F, Kessaris N, Alvarez-Buylla A, Richardson WD, Rowitch DH. Regional astrocyte allocation regulates CNS synaptogenesis and repair. Science. 2012;337(6092):358-62.
3. Shao W, Zhang S, Tang M, Zhang X, Zhou Z, Yin Y, Zhou Q, Huang Y, Liu Y, Wawrousek E, Chen T, Li S, Xu M, Zhou J, Hu G, Zhou J. Suppression of neuroinflammation by astrocytic dopamine D2 receptors via αB-crystallin. Nature. 2013;494 (7435):90-4.
4. Tan EK, Chao YX, West A, Chan LL, Poewe W, Jankovic J. Parkinson disease and the immune system - associations, mechanisms and therapeutics. Nat Rev Neurol. 2020;16 (6):303-18.
5. Voitenko LP, Nikonenko AG. Modification of experimental rotenone model of Parkinson's disease. Fiziol Zh. 2015;61(1):83-90. [Ukrainian].
6. Rodgers KR, Lin Y, Langan TJ, Iwakura Y, Chou RC. Innate immune functions of astrocytes are dependent upon tumor necrosis factor-alpha. Sci Rep. 2020;10(1):7047.
7. Burda JE, Bernstein AM, Sofroniew MV. Astrocyte roles in traumatic brain injury. Exp Neurol. 2016; 275 (Part 3):305-15.
8. Khakh BS, Sofroniew MV. Diversity of astrocyte functions and phenotypes in neural circuits. Nat Neurosci. 2015;18 (7):942-52.
9. Ge WP, Miyawaki A, Gage FH, Jan YN, Jan LY. Local generation of glia is a major astrocyte source in postnatal cortex. Nature. 2012;484(7394):376-80.
10. Peng H, Long F, Zhou J, Leung G, Eisen MB, Myers EW. Automatic image analysis for gene expression patterns of fly embryos. BMC Cell Biol. 2007;8 (Suppl 1):S7.
11. Longair MH, Baker DA, Armstrong JD. Simple neurite tracer: open source software for reconstruction, visualization and analysis of neuronal processes. Bioinformatics. 2011;27:2453-4.

12. Basu S, Dahl KN, Rohde GK. Localizing and extracting filament distributions from microscopy images. J Microsc. 2015;258 (1):13-23.

13. Bogdaniuk AO, Nikonenko AG. Spatial dimension of nigral astroglyosis observed in rotenone model of Parkinson's disease. Fiziol Zh. 2018;64(6): 40-6.

Received 28.06.2022